Pharmaceutical Sciences Asia

Pharm Sci Asia 2019; 46 (3), 156-162

DOI: 10.29090/psa.2019.03.018.0043

Research Article

Preliminary *in vitro* permeability, cytotoxicity and cardiotoxicity evaluation of triazole-quinuclidine T6

Kuntarat Arunrungvichian[1*], Putthiporn Khongkaew[1,2], Sununta Panyasang[1], Jiradanai Sarasamkan[3]

[1]Department of Pharmaceutical Chemistry, Faculty of Pharmacy, Mahidol University, 447 Sri-Ayudha Road, Bangkok 10400, Thailand
[2]Faculty of Pharmaceutical Science, Burapha University, 169 Long-haad Bangsaen Road, Saensook, Mueng, Chonburi 20131, Thailand
[3]National Cyclotron and PET Centre, Chulabhorn Hospital, 54 Kamphaeng Phet 6 Road, Bangkok 10210, Thailand

*Corresponding author:
Kuntarat Arunrungvichian
kuntarat.aru@mahidol.edu

KEYWORDS:
T6; Cytotoxicity; Cardiotoxicity; Permeability

ABSTRACT

The permeability and safety of two lead compounds, (*R*)-T6 and (*S*)-T6, which are selective nicotinic acetylcholine receptor (nAChR) ligands for α7 nAChR and α3β4 nAChR, respectively, were evaluated *in vitro* to provide support to move on to preclinical studies. The α7 nAChR is well recognized as a drug target for neurodegenerative diseases while that of α3β4 nAChR is for drug addiction. The permeability of (*R*)-T6 and (*S*)-T6 assessed by parallel artificial membrane permeability assay (PAMPA) indicated high human oral absorption with effective permeability (P_e) of 2.47×10^{-6} and 8.99×10^{-6} cm/s, respectively. The cytotoxicity and the cardiotoxicity were determined to assess the safety of (*R*)-T6 and (*S*)-T6. The cytotoxic IC_{50} values of (*R*)-T6 and (*S*)-T6 on normal HEK 293 cells obtained by MTT assays were 24.98 and 90.93 μM, respectively. For cardiac-safety test, the effect on human ether-a-go-go-related gene (hERG) potassium channels was determined by fluorescence polarization-based assay, the result suggested that (*R*)-T6 and (*S*)-T6 bind to hERG potassium channel but in the same level with the common drugs such as haloperidol and thioridazine. Collectively, (*R*)-T6 and (*S*)-T6 exhibited favorable permeability and acceptable safety profile. These preliminary data support the safety and suitability of the (*R*)-T6 and (*S*)-T6 to proceed to preclinical animal studies.

1. INTRODUCTION

A nAChR is a member of Cys-loop ligand-gated ion channel superfamily composed of five subunits surrounding an ion pore. There are at least 12 neuronal subunits which are α2-α10 and β2-β4 characterized in human and avian systems [1,2]. The localization and stoichiometry difference of nAChRs lead to functional and pharmacological variance [3,4]. The important nAChRs found in brain are α7, α4β2 and α3β4 subtypes. The α7 and α4β2 subtypes have the highest expression level in cerebral cortex and hippocampus associated with cognition, memory and behavior [5]. The α7 and α4β2 subtypes are important drug targets for neurodegenerative diseases including Alzheimer's disease, cognitive deficits of schizophrenia, attention-deficit hyperactivity disorder (ADHD) and Parkinson's disease [6-8]. The α3β4 nAChR has been implicated in substance addiction and depression, the α3β4

https://:www.pharmacy.mahidol.ac.th/journal/
© Faculty of Pharmacy, Mahidol University (Thailand) 2018

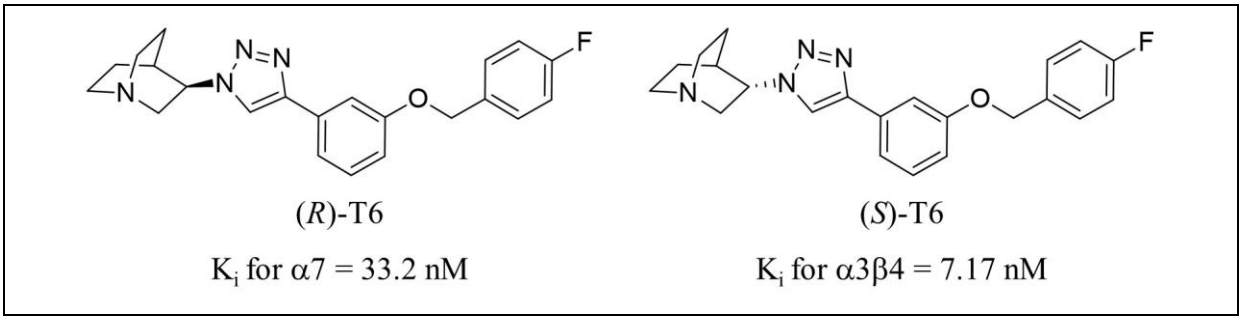

Figure 1. Chemical structures and *in vitro* binding affinity of (*R*)-T6 and (*S*)-T6.

subtype is mainly expressed in autonomic ganglia and some brain regions i.e. medial habenula, nucleus interpeduncularis, dorsal medulla, and pineal gland [9].

According to the potential of α7 and α3β4 nAChRs as drug targets, a number of compounds with different chemotypes have been developed to act on these targets. For instance, several triazole-containing molecules and triazole-quinuclidine compounds have been previously reported as α7, α4β2 and α3β4 nAChR ligands [10-13]. Recently, the selective binding of triazole-quinuclidine compounds to the nAChR subtypes was reported to be governed by the stereocenter at position 3 of quinuclidine scaffold. The (*R*)-enantiomers showed subtype selectivity for α7 nAChR, whereas the (*S*)-enantiomers predominantly binds to α3β4 nAChR. (*R*)- and (*S*)- enantiomers of compound T6 (Figure 1) are the promising lead compounds based on the high selectivity and affinity. (*R*)-T6 has high affinity to α7 nAChR (K_i 33.2 nM) and selective for α7 nAChR over α3β4 (33 fold) and α4β2 subtypes (193 fold), whereas (*S*)-T6 having high affinity to α3β4 subtype with K_i of 7.17 nM, is selective to α3β4 nAChR over α7 and α4β2 subtypes 21 and 75 fold, respectively [13].

Herein, the preliminary studies on the permeability and toxicity of the enantiomers of compound T6 were carried out to provide data to support further preclinical studies in animal models.

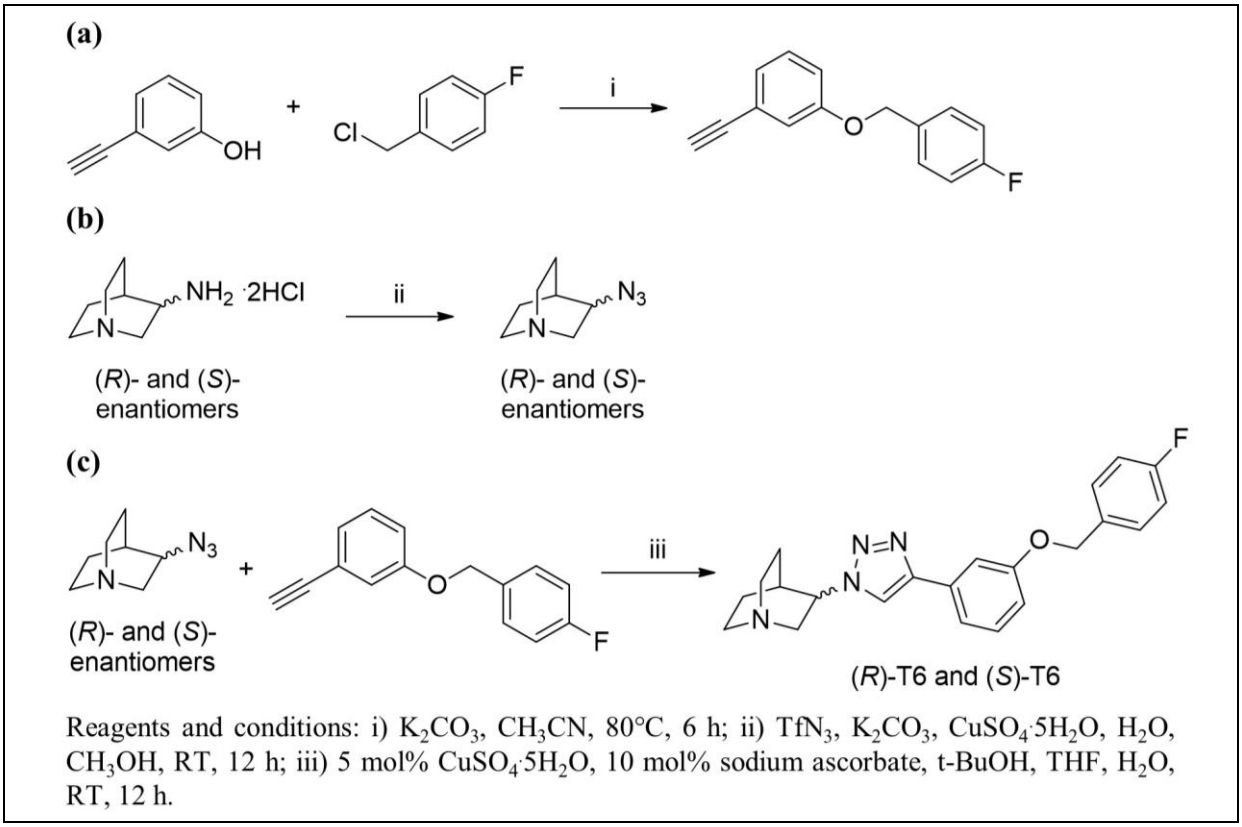

Scheme 1. Synthesis of terminal alkyne **(a)**, azide **(b)**, and (*R*)- and (*S*)-T6 **(c)**.

2. MATERIALS AND METHODS

2.1. Test compounds T6

(*R*)-T6 and (*S*)-T6 were synthesized by the previously described method [13]. In brief, the terminal alkyne and quinuclidine azide were prepared at first before reacting these two prepared reagents with click chemistry to yield triazole-quinuclidine compound. For the alkyne part, 4-fluorobenzyl chloride was reacted with 3-hydroxyphenylacetylene and K_2CO_3 in acetonitrile at 80 °C for 6 h (Scheme 1a) and purified by SiO_2 column chromatography using $CHCl_3$/hexane (50/50) as a mobile phase to yield 1-ethynyl-3-((4-fluorobenzyl)oxy)benzene as pale colorless oil. For the (*R*)- and (*S*)-quinuclidine azides, trifluoromethanesulfonic anhydride was added dropwise into a solution of sodium azide in the mixed solvent of water and toluene. The reaction mixture was vigorously stirred at 0 °C for 2 h and extracted with toluene to yield trifluoromethanesulfonylazide (TfN_3). The freshly prepared TfN_3 in toluene was added into the reaction mixture of (*R*) or (*S*) of 3-aminoquinuclidine dihydrochloride, K_2CO_3, $CuSO_4{\cdot}5H_2O$ in water and methanol and was vigorously stirred at room temperature for 12 h (Scheme 1b). After that, it was poured into water and extracted with CH_2Cl_2 before washing with brine solution and drying over anhydrous Na_2SO_4. The solvent was removed under reduced pressure to yield (*R*)-azidoquinuclidine and (*S*)-azidoquinuclidine as yellow liquid and used without purification.

To obtain the target triazole-quinuclidine T6, 1-ethynyl-3-((4-fluorobenzyl)oxy)benzene in t-BuOH was added into (*R*)-azidoquinuclidine or (*S*)-azidoquinuclidine in THF. Then, $CuSO_4{\cdot}5H_2O$ and sodium ascorbate in water were added and stirred at room temperature for 12 h (Scheme 1c) before extracted with CH_2Cl_2. The organic layer was washed with brine solution and dried over anhydrous Na_2SO_4. The solvent was removed under reduced pressure and purified by SiO_2 column chromatography using MeOH/CH_2Cl_2 (20/80) as a mobile phase to yield *(R)*-T6 and *(S)*-T6 as a white solid.

2.2. Permeability test [14]

The permeability of test compound was evaluated by parallel artificial membrane permeability assay (PAMPA) (Corning, USA). The Corning Gentest™ Pre-coated PAMPA Plate System (Cat. No. 353015) which composed of a 96-well plate/insert system was used to perform the permeability assays. Two compartments (donor and receiver wells) are separated by a polyvinylidene fluoride (PVDF) plate pre-coated with a phospholipid-oil-phospholipid tri-layer consisting of DOPC phospholipids. Test compounds were prepared as 10 mM stock concentration in DMSO and diluted to 200 μM working solution with phosphate buffer solution (PBS), pH 7.4. The test compound (300 μL) was added to a receiver plate. Then, PBS (200 μL) was added into a filter plate before placing the filter plate on the receiver plate. The plate was incubated at 25 °C for 5 h. After that, the plates were separated. The 150 μL of solutions from each well of the receiver and filter plates were drawn to analyze by microplate reader (CLARIOstar, Germany) using UV-transparent plates (Corning, USA).

The permeability (cm/s) was calculated using the following formula:

$$\text{Permeability } (P_e) = [-\ln[1-C_A(t)/C_{eq}]]/[A*(1/V_D+1/V_A)*t]$$

where V_D = donor well volume (0.3 mL), V_A = acceptor well volume (0.2 mL), A = filter area (0.3 cm^2), t = incubation time (seconds), $C_A(t)$ = compound concentration in acceptor well at time t, $C_D(t)$ = compound concentration in donor well at time t, $C_{eq} = [(C_D(t)xV_D)+(C_A(t)xV_A)]/(V_D+V_A)$.

2.3. Cytotoxicity test [15]

The cytotoxicity test in human embryonic kidney cells 293 (HEK 293 cells) was tested by MTT assay, which is a colorimetric assay. Briefly, cells suspension in DMEM containing 10% FBS and 1% penicillin/streptomycin were seeded into 96 well plate (3 x 10^4 cells/90 μL/well) and incubated at 37 °C for 24 h. Then, test compounds (10 μL) were added and further incubated for 48 h. The final concentration of DMSO is 1%. After that, the treated medium was replaced with 100 μL of PBS containing 0.05% w/v of MTT solution. After 4 h of incubation, the medium was discarded and 100 μL of DMSO was added. The plate was then shaken for 20 min. The absorbance was measured by a spectrophotometric

microplate reader (Tecan, Switzerland) at 570 nm. All compounds were tested in 1-10,000 μM range. 1% DMSO and verapamil were used as a control and a positive control, respectively. All test compounds were performed in duplicate of three experiments. The IC_{50} was analyzed by GraphPad Prism 5 software using nonlinear regression analysis to construct a dose-response curve. The test compound concentration was transformed to log form, whereas the response was plotted in linear scale.

2.4. Cardiotoxicity test [16]

The cardiotoxicity was evaluated by using Predictor™ hERG fluorescence polarization assay kit (SelectScreen™ Biochemical hERG Screening Service, ThermoFisher Scientific, USA). Briefly, the stock solution of test compounds was prepared by dilution with assay buffer (25 mM HEPES (pH 7.5), 15 mM KCl, 1 mM $MgCl_2$, and 0.05% Pluronic F-127) to obtain 3-fold serial dilutions of test compounds for 10-point titrations. The highest concentration of test compound was 10 μM. Each concentration of test compound (5 μL) was added into an assay plate (384 well untreated low-volume polystyrene microplates) in the absence and presence of potent hERG ligand E-4031 (30 μM final concentration). Then, 10 μL of hERG Membranes was added followed by 5 μL of hERG Tracer Red (1 nM final concentration). The assay plate was mixed on a shaker for 20-30 seconds before covering the plate and incubation for 3 h at room temperature. The assay plate was read on a fluorescence plate reader (Tecan Safire, Switzerland). The excitation and emission values were set at 530 and 585 nm, respectively and the bandwidth was set at 20 nm. The dose response curve was analyzed by using XL*fit* from IDBS. The assay was run in duplicate and the IC_{50} was reported.

3. RESULTS AND DISCUSSION

The *in vitro* studies on permeability and safety profiles of two potential lead compounds (*R*)-T6 and (*S*)-T6 acting on α7 and α3β4 nAChRs, respectively were conducted to provide the preliminary data for entering preclinical study in animal models. The *in vitro* permeability and safety profiles established in the very early stages are essential to reduce drug attrition in the preclinical and late stages of clinical trials.

One of the most important factor of pharmacokinetic parameters is absorption. Several drugs have failed in clinical studies due to absorption problem [17]; therefore, the prediction of gastrointestinal (GI) permeability of drugs is required in early drug discovery to assess oral-absorption potential of drug candidates. A non-cell based assay, PAMPA was employed to predict the *in vivo* passive absorption of the target compounds, (*R*)- and (*S*)- enantiomers. An artificial PVDF membrane pre-coated with structured layers of phospholipids was applied to simulate lipid bilayer of intestinal epithelial cells in PAMPA model. This *in vitro* model was selected to measure a compound's passive permeability during lead identification before the preclinical phase because the PAMPA assay is simple, rapid, low-cost and robust compared to the labor-intensive and expensive conventional cell-based assay [18,19]. However, the cell-based assays such as Caco-2 cells and Mardin-Darby canine kidney (MDCK) as well as *in vivo* studies are still required in the later preclinical phase to provide additional information on the carrier-mediated transports in the absorption process and metabolism despite the lack of CYP3A4 and low expression of metabolic enzymes and transporters in Caco-2 and MDCK cell lines [20,21]. Despite the lack of transporters and metabolic enzymes, the PAMPA permeability values appeared to be in good agreement with the Caco-2 and human absorption values [21]. The PAMPA permeability P_e values of (*R*)-T6 and (*S*)-T6 are 2.47 x 10^{-6} and 8.99 x 10^{-6} cm/s, respectively (Table 1), which are greater than 1.5 x 10^{-6} cm/s indicating the high permeability [14]. These data suggested the good oral absorption of (*R*)-T6 and (*S*)-T6.

Another factor causing drug failure in clinical trials is a safety profile [17] that (*R*)-T6 and (*S*)-T6 were evaluated for cytotoxicity and cardiotoxicity. The *in vitro* cytotoxicity test in normal HEK 293 cells was performed at first by MTT assay to evaluate the safety of (*R*)-T6 and (*S*)-T6 before proceeding to the efficacy test in

Table 1. *In vitro* permeability and toxicity profiles of (*R*)-T6 and (*S*)-T6.

	(*R*)-T6	(*S*)-T6
Permeability (P_e, x 10^{-6} cm/s)	2.47 ± 4.16	8.99 ± 1.56
Cytotoxicity (IC_{50}, μM)	24.98 ± 10.74	90.93 ± 8.98
Cardiotoxicity (IC_{50}, nM)	486	120

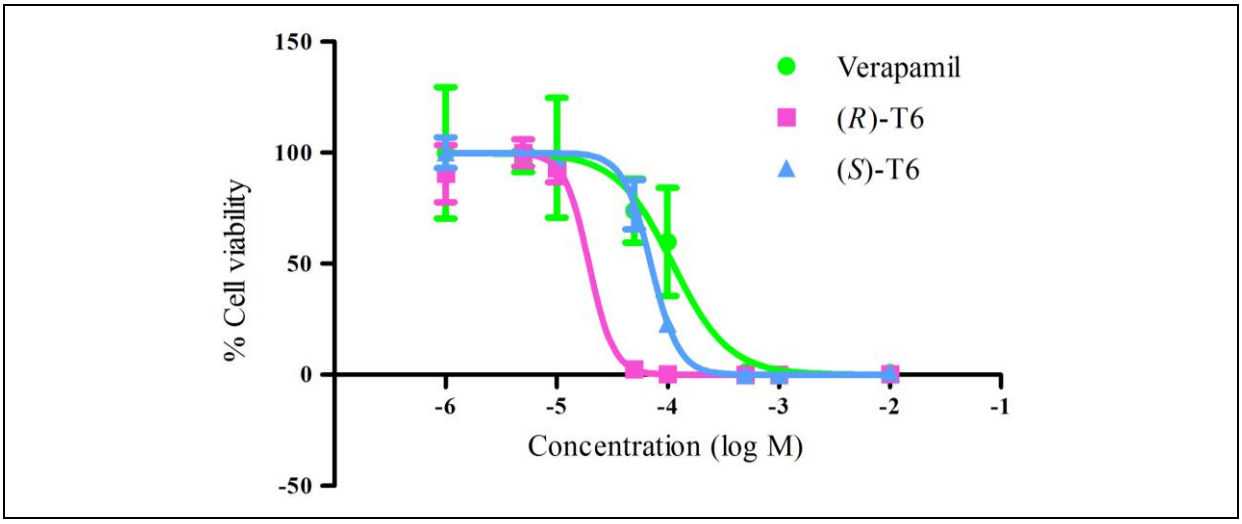

Figure 2. Dose-response curve of (*R*)-T6 and (*S*)-T6 in cytotoxicity test.

the animal models. The 50% inhibition concentrations (IC_{50}) of (*R*)-T6 and (*S*)-T6 are 24.98 and 90.93 μM, respectively (Table 1, Figure 2). The IC_{50} values of these two compounds are in micromolar range as verapamil (IC_{50} = 111.9 μM), which is a drug used in a human, indicating the safety profile to normal cells of (*R*)-T6 and (*S*)-T6.

For the cardiotoxicity, a compound that is able to block hERG K^+ channel tends to cause cardiotoxicity from QT prolongation, which may develop potentially lethal 'torsades-de-pointes' (TdP) arrhythmias leading to sudden death [22]. Hence, the assessment of hERG K^+ channel is required before starting clinical studies and consequently, the *in vitro* assays to screen the lead compounds for activity on hERG K^+ channel is performed early in the lead identification process to reduce the risk of failing in the preclinical study due to the adverse cardio-vascular effects, particularly the most serious Tdp *in vivo*. A number of hERG assays to assess cardiac safety have been developed e.g. patch clamp electrophysiology, radioligand binding assay, liposome flux assay, fluorescence polarization-based (FP) assays [17,23-27]. The hERG FP assay was selected because FP assay is fast, simple, inexpensive, reliable, and inexposure to radiation. Nonetheless, the binding data for hERG channel obtained from FP assay showed high correlation to the traditional methods, patch clamp electrophysiology and radioligand binding data [16]. In FP assay, a plane of polarized light will excite a fluorescent tracer molecule such as fluorescein, Texas Red, BODIPY, Cy5 and rhodamines, the polarization of the emitted light will be retained in case a tracer still bound to hERG K^+ channel. If a test compound can bind to hERG K^+ channel, light emission from tracer will be depolarized [16]. This method detects a change of a signal occurred when a compound displaces a fluorescence probe binding to hERG K^+ channel. In the assay, (*R*)-T6 and (*S*)-T6 were firstly tested for the polarization and fluorescence interference and no interference of test compounds from non-specific interaction was observed neither to polarization nor fluorescence values. The IC_{50} of (*R*)-T6 and (*S*)-T6 to hERG K^+ channel is 486 and 120 nM, respectively (Table 1, Figure 3), whereas the IC_{50} of E-4031, a selective hERG K^+ channel inhibitor is 12.5 nM. The IC_{50} of these two compounds to hERG K^+ channel are in nanomolar range indicating the high binding to hERG channel, but the IC_{50} values are 3.6-14.7 fold higher than the reported values of terfenadine (IC_{50} = 33 nM)[16], a well-known withdrawn anti-histamine because of cardiotoxicity[26], and comparable to antipsychotic drugs, haloperidol (IC_{50} = 187 nM) and thioridazine (IC_{50} = 655 nM)[16]. As FP hERG assay is a nonfunctional assay and a possibility of false-positive, the functional cell-based assay and the gold standard electrophysiology assay need to be conducted to confirm hERG safety of (*R*)-T6 and (*S*)-T6. In addition, the clinical QT interval prolongation will not occur if hERG IC_{50} is 30-fold higher than the therapeutic plasma concentration [28]. The further *in vivo* experiment to get the effective therapeutic plasma concentration should be performed to confirm a safety margin of (*R*)-T6 and (*S*)-T6.

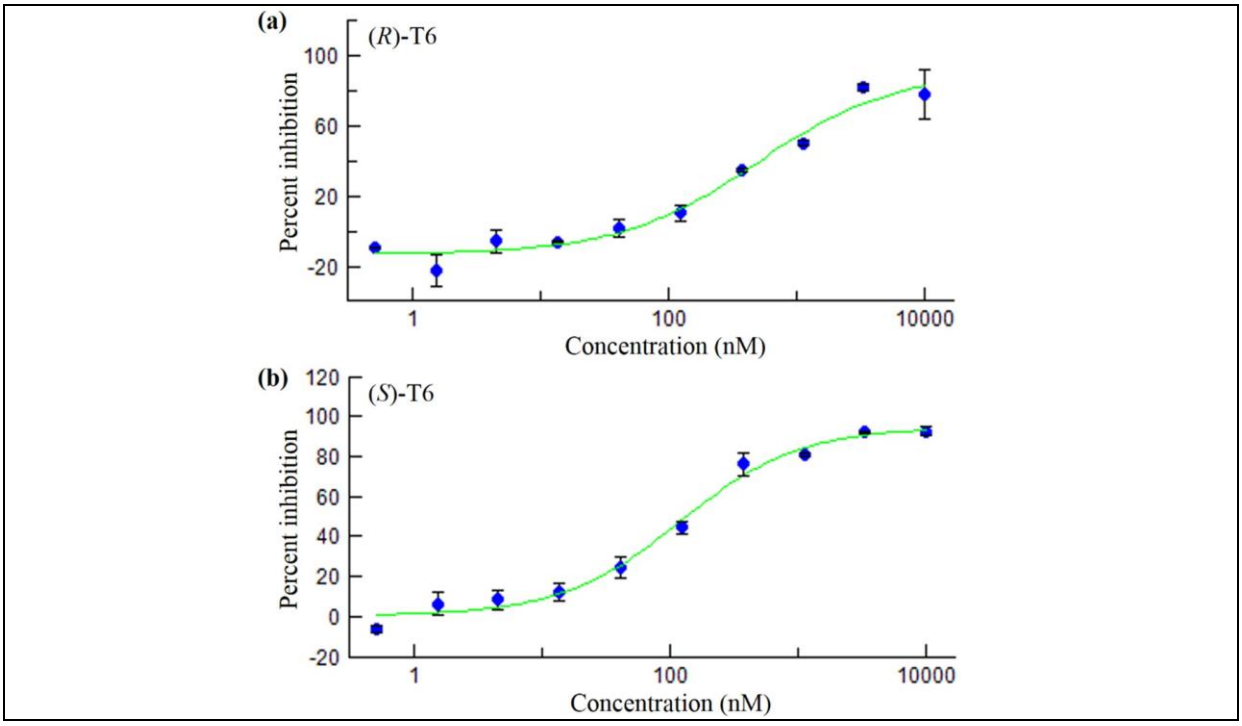

Figure 3. Dose-response curve of (*R*)-T6 **(a)** and (*S*)-T6 **(b)** in hERG safety assay.

4. CONCLUSIONS

(*R*)-T6 and (*S*)-T6 which are potent and selective α7 and α3β4 nAChR ligands, respectively can proceed to preclinical studies in animal models on account of the obtained preliminary data showing good permeability and acceptable safety profiles. However, the assessment of cardiotoxicity by other assays needs to be carried out to confirm the safety profile of these two compounds.

5. ACKNOWLEDGEMENTS

Conflict of interest
There is no conflict of interest.

Funding
This research project is supported by Mahidol University.

Ethical approval
None to declared

Article info:
Received August 25, 2018
Received in revised form September 25, 2018
Accepted September 28, 2018

REFERENCES

1. Gotti C, Zoli M, Clementi F. Brain nicotinic acetylcholine receptors: native subtypes and their relevance. Trends Pharmacol Sci. 2006;27(9):482-91.
2. Jensen AA, Frolund B, Liljefors T, Krogsgaard-Larsen P. Neuronal nicotinic acetylcholine receptors: structural revelations, target identifications, and therapeutic inspirations. J Med Chem. 2005;48(15):4705-45.
3. Lippiello P, Bencherif M, Hauser T, Jordan K, Letchworth S, Mazurov A. Nicotinic receptors as targets for therapeutic discovery. Expert Opin Drug Discov. 2007;2(9):1185-203.
4. Gaimarri A, Moretti M, Riganti L, Zanardi A, Clementi F, Gotti C. Regulation of neuronal nicotinic receptor traffic and expression. Brain Res Rev. 2007;55(1):134-43.
5. Lindstrom JM. Nicotinic acetylcholine receptors of muscles and nerves: comparison of their structures, functional roles, and vulnerability to pathology. Ann N Y Acad Sci. 2003;998:41-52.
6. Dani JA, Bertrand D. Nicotinic acetylcholine receptors and nicotinic cholinergic mechanisms of the central nervous system. Annu Rev Pharmacol Toxicol. 2007;47:699-729.
7. Toyohara J, Hashimoto K. Alpha7 Nicotinic Receptor Agonists: potential therapeutic drugs for treatment of cognitive impairments in schizophrenia and Alzheimer's disease. Open Med Chem J. 2010;4:37-56.
8. Wilens TE, Decker MW. Neuronal nicotinic receptor agonists for the treatment of attention-deficit/ hyperactivity disorder: focus on cognition. Biochem Pharmacol. 2007;74(8):1212-23.
9. Gotti C, Clementi F, Fornari A, Gaimarri A, Guiducci S, Manfredi I, et al. Structural and functional diversity of native brain neuronal nicotinic receptors. Biochem Pharmacol. 2009;78(7):703-11.
10. Yamauchi JG, Gomez K, Grimster N, Dufouil M, Nemecz A, Fotsing JR, et al. Synthesis of selective agonists for the α7 nicotinic acetylcholine receptor with in situ click-chemistry on acetylcholine-binding protein templates. Mol Pharmacol. 2012;82(4):687-99.

11. Arunrungvichian K, Fokin VV, Vajragupta O, Taylor, P. Selectivity optimization of substituted 1,2,3-triazoles as α7 nicotinic acetylcholine receptor agonists. ACS Chem Neurosci. 2015;6(8):1317-1330.
12. Arunrungvichian K, Boonyarat C, Fokin VV, Taylor P, Vajragupta O. Cognitive improvements in a mouse model with substituted 1,2,3-triazole agonists for nicotinic acetylcholine receptors. ACS Chem Neurosci. 2015;6(8):1331-1340.
13. Sarasamkan J, Scheunemann M, Apaijai N, Palee S, Parichatikanond W, Arunrungvichian K, et al. Varying chirality across nicotinic acetylcholine receptor subtypes: selective binding of quinuclidine triazole compounds. ACS Med Chem Lett. 2016;7(10):890-895.
14. Chen X, Murawski A, Patel K, Crespi CL, Balimane PV. A novel design of artificial membrane for improving the PAMPA model. Pharm Res. 2008;25(7):1511-20.
15. Ahmad JL, Okebaram CC, Samaila A. Cytotoxic effect of verapamil on human embryonic kidney cell line. IJSTR. 2016;5(12):83-87.
16. Piper DR, Duff SR, Eliason HC, Frazee WJ, Frey EA, Fuerstenau-Sharp M, et al. Development of the predictor hERG fluorescence polarization assay using a membrane protein enrichment approach. Assay Drug Dev Technol. 2008;6(2):213-23.
17. Pritchard JF, Jurima-Romet M, Reimer ML, Mortimer E, Rolfe B, Cayen MN. Making better drugs: Decision gates in non-clinical drug development. Nat Rev Drug Discov. 2003;2(7):542-53.
18. Avdeef A, Artursson P, Neuhoff S, Lazorova L, Grasjo J, Tavelin S. Caco-2 permeability of weakly basic drugs predicted with the double-sink PAMPA pKa(flux) method. Eur J Pharm Sci. 2005;24(4):333-49.
19. Avdeef A, Bendels S, Di L, Faller B, Kansy M, Sugano, K, et al. PAMPA--critical factors for better predictions of absorption. J Pharm Sci. 2007;96(11):2893-909.
20. Awortwe C, Fasinu PS, Rosenkranz B. Application of Caco-2 cell line in herb-drug interaction studies: current approaches and challenges. J Pharm Pharm Sci. 2014;17(1):1-19.
21. Lennernas H. Regional intestinal drug permeation: biopharmaceutics and drug development. Eur J Pharm Sci. 2014;57:333-41.
22. Vandenberg JI, Perry MD, Perrin MJ, Mann SA, Ke Y, Hill AP. hERG K(+) channels: structure, function, and clinical significance. Physiol Rev. 2012;92(3):1393-478.
23. Finlayson K, Turnbull L, January CT, Sharkey J, Kelly JS. [3H]dofetilide binding to HERG transfected membranes: a potential high throughput preclinical screen. Eur J Pharmacol. 2001;430(1):147-8.
24. Chiu PJ, Marcoe KF, Bounds SE, Lin CH, Feng JJ, Lin A, et al. Validation of a [3H]astemizole binding assay in HEK293 cells expressing HERG K+ channels. J Pharmacol Sci. 2004;95(3):311-9.
25. Su Z, Brown EC, Wang W, MacKinnon R. Novel cell-free high-throughput screening method for pharmacological tools targeting K+ channels. PNAS. 2016;113(20):5748-53.
26. Danker T, Moller C. Early identification of hERG liability in drug discovery programs by automated patch clamp. Front Pharmacol. 2014;5:203.
27. Priest BT, Bell IM, Garcia ML. Role of hERG potassium channel assays in drug development. Channels. 2008;2(2):87-93.
28. Redfern WS, Carlsson L, Davis AS, Lynch WG, MacKenzie I, Palethorpe S, et al. Relationships between preclinical cardiac electrophysiology, clinical QT interval prolongation and torsade de pointes for a broad range of drugs: evidence for a provisional safety margin in drug development. Cardiovasc Res. 2003;58(1):32-45.